Temperature Profile of Hotspots in Narrow Current-Biased Superconducting Strips

J. P. Maneval, K. Harrabi, F. Chibane, M. Rosticher, F. R. Ladan, and P. Mathieu

***Abstract*—The one-dimensional heat flow equation controlling the temperature of a current-driven hotspot (HS) in a long superconducting microbridge is reexamined in all its components. The resulting nonlinear differential system, which admits temperature-dependent thermal conductivities, and a blackbody-like phonon radiation into the substrate, is solved numerically. In this work, the phonon escape rate is not the outcome of a best-fitting procedure, but rather is derived from the dependence, in a pulse experiment, of the HS nucleation time upon the current intensity. As a result, the temperature profile of a self-heating HS in a niobium strip can be computed *without any adjustable parameter* for each choice of the bath temperature. One notes a severe limitation of the HS temperature as compared to previous models. The minimum current sustaining a stable HS thus determined is in close agreement with direct measurements even far from the critical temperature. The method is applied to a NbN filament typical of the superconducting single photon detectors.**

***Index Terms*—Nanowires, superconducting photodetectors, superconducting thin films, thin film sensors.**

I. Introduction

THE FORMATION of a hotspot (HS) and the dynamics of its subsequent elimination form an essential part of the detection process in many thin-film devices, such as the Nanowire-Superconducting Single Photon Detectors (N-SSPDs) [1]. However, the temperature reached locally as well as the timing jitter can only be described qualitatively. In this respect, the simpler problem of a hotspot initiated and sustained by an electrical current may be a useful approach. Skocpol *et al.* [2] calculated the temperature T(x) as a function of the position x in the linear approximation of heat transfer to the external heat bath. Several improvements [3], [4] in the heat transfer coefficients allowed extending the validity of the treatment for bath temperatures T_0 far from T_c, the critical temperature. Since T(x) cannot be probed directly (apart exceptions), a comparison between theory and experiment bears on $I_h(T_0)$, the minimum HS current. That procedure usually leaves arbitrary the heat transfer coefficient through the film-to-substrate interface.

In the present work, we take full account of the non-linear heat flow relations, and treat the case of niobium strips sputtered on sapphire [5], for which all the relevant parameters have been determined independently. Then the comparison of the computed $I_h(T_0)$ with experimental data can be performed in absolute terms.

II. From Linear Heat Transfer to T-Dependent Thermal Coefficients

A. Small Temperature Deviation (STD) Model [2]

A uniform strip of width w, engraved in a film of thickness b, carries a fixed electrical current I (or equivalently a current density per unit area $J = I/wb$). We also denote by C the specific heat per unit volume of the film, by κ its volumic heat conductivity coefficient, by ρ its electrical resistivity, and by α the coefficient per unit area of linear heat transfer to the thermal bath. The general energy rate equation in one dimension reads:

$$\frac{d}{dx}\left[\kappa \frac{dT}{dx}\right] + \rho J^2 - \frac{\alpha}{b}(T - T_0) = 0. \tag{1}$$

The common way to deal with hotspots is the stepwise heat generation model, in which the Joule power density switches from the normal (N) state value ρJ^2 where $T > T_c$, to zero when passing to a (S) region (perfectly resistanceless $\rho = 0$). The condition of HS stability implicit in (1) fixes J at a unique value, that we call J_h.

B. A Solitary Solution

What we consider in this work are spatially-limited (solitary) structures. The origin $x = 0$ is chosen on the left front of the hotspot (Fig. 1), where T(x) passes through the transition temperature T_c. A step-like solution joining the S and N zone will be composed of $T_S(x < 0)$ and $T_N(x > 0)$ satisfying respectively:

$$\text{For} \quad x < 0 \quad T_S(x) - T_0 = (T_c - T_0)\exp(x/\eta_S) \tag{2a}$$

$$\text{For} \quad x > 0 \quad T_M - T_N(x) = (T_M - T_c)\exp(-x/\eta_N) \tag{2b}$$

where $\eta_S = (\kappa_S b/\alpha)^{1/2}$ and $\eta_N = (\kappa_N \beta/\alpha)^{1/2}$ are the thermal healing lengths for the S and N zones respectively. The heat generation term ρJ^2 has been absorbed in the HS asymptotic temperature T_M, determined by the continuity of the heat flux

Manuscript received October 9, 2012; accepted December 12, 2012. Date of publication December 20, 2012; date of current version January 25, 2013. This work was supported in part by KFUPM, Dharhan, Saudi Arabia, under Contract IN 100034-DSR.

J. P. Maneval, M. Rosticher, and P. Mathieu are with Laboratoire Pierre Aigrain, Ecole Normale, 75231 Paris, France (e-mail: maneval@lpa.ens.fr; michael.rosticher@ens.fr; patrice.mathieu@lpa.ens.fr).

K. Harrabi is with the Physics Department, King Fahd University for Petroleum and Minerals, Dharhan 31261, Saudi Arabia (e-mail: harrabi@kfupm.edu.sa).

F. Chibane is with Faculté des Sciences, Université Ibnou Zohr, 80000 Agadir, Morocco (e-mail: fa_chibane@hotmail.com).

F. R. Ladan is with the Department of Physics, Ecole Normale, 75231 Paris, France (e-mail: ladan@ens.fr).

Color versions of one or more of the figures in this paper are available online at http://ieeexplore.ieee.org.

Digital Object Identifier 10.1109/TASC.2012.2235507

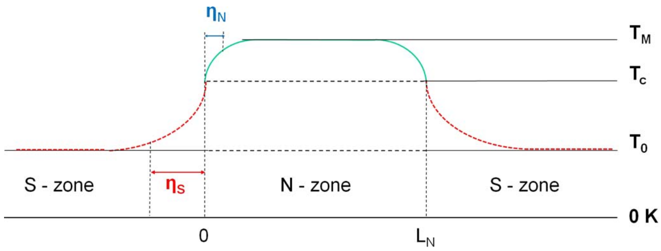

Fig. 1. Schematic temperature profile of a steady solitary HS showing an extendable central part bordered by healing lengths on each side. The Joule heat generated in the N-zone above $T_{\rm c}$ is released (i) by diffusion along the filament and (ii) by contact with the cryogenic bath at T_0.

at $x = 0$. The unicity of $T_{\rm M}$, and of the corresponding $J = J_{\rm h}$, results from the condition of HS stability.

C. Blackbody-Type Phonon Radiation, Plus T-Dependent Heat Conductivities

For limited temperature departures from $T_{\rm c}$, typically 0.9 $T_{\rm c} < T_0 < T_{\rm c}$, the STD model generally describes correctly the experimental data on $J_{\rm h}(T_0)$ defined by (1), provided that the heat transfer coefficient is treated as an adjustable constant. However, Yamasaki and Aomine [3] found it possible to encompass a much wider temperature range by replacing the linear form $\alpha(T - T_0)$ by the quartic thermal transfer term:

$$A\left(T^4 - T_0^4\right) \tag{3}$$

by similarity with the Kapitza heat transfer with the liquid helium bath. They solved the heat flow (1) numerically to provide a temperature profile T(x) of a self-heating HS in granular-Al strips. By adjustment of the coefficient A (typically 25 W.K^{-4}.m^{-2}), they obtained a good fit of their $J_{\rm h}$ vs T_0 data down to about 0.7 $T_{\rm c}$. Elaborating on that “modified SBT model”, Dharmadurai & Satya Murthy [4] introduced T-dependent heat conductivities $\kappa_{\rm S} \sim T^3$ and $\kappa_{\rm N} \sim T$, each defined within an adjustable proportionality constant (DSM model).

III. Fully Temperature-Dependent (FTD) Parameters

A. Differential Equations

Our approach embodies the above ingredients, with the important difference that the heat conductivities, as well as the coefficient A, derive from independent measurements (see [8]). If the electron heat conductivities are developed according to $\kappa_{\rm S} = D_{\rm e}C_{\rm eS}$ and $\kappa_{\rm N} = D_{\rm e}C_{\rm eN}$, where $C_{\rm eS}$ and $C_{\rm eN}$ are the electronic specific heats in the S and N state respectively, and $D_{\rm e}$ is the electron diffusion constant, assumed to be invariable throughout, the derivative present in (1) splits into two terms:

$$\frac{d}{dx}\left[\kappa(T)\frac{dT}{dx}\right] = D_e C_e(T)\frac{d^2T}{dx^2} + D_e\frac{dC_e}{dT}\left[\frac{dT}{dx}\right]^2. \tag{4}$$

(The second term, in $(dT/dx)^2$, was omitted in [4] with no justification, although it is of magnitude comparable to the first one). From now on, the specific heats previously introduced will be written under the forms: $C_{\rm eS} = \mu T^3$; $C_{\rm eN} = \gamma T$, plus $C_\varphi = \beta T^3$ for the phonon specific heat in the Debye model. Upon renaming of the surface transfer coefficient in the form $A = \alpha/4T_{\rm c}^3 = b\beta/4\tau$, which implies that τ is a characteristic decay time, to be explicited soon, one preserves the consistency with the linear case near $T_{\rm c}$. The couple of differential equations governing a steady-state HS then becomes:

$$x<0\ T_S^3\frac{d^2T_s}{dx^2}+3T_S^2\left(\frac{dT_S}{dx}\right)^2=(1/4\eta_s^2)[T_S^4-T_0^4] \tag{5a}$$

$$x>0\ T_c^2T_N\frac{d^2T_N}{dx^2}+T_c^2\left(\frac{dT_N}{dx}\right)^2=(1/4\eta_N^2)[T_M^4-T_N^4]\,. \tag{5b}$$

$T_{\rm M}$, that coincides with the HS temperature reached asymptotically at $x = +\infty$, is given by:

$$\rho J_h^2 = \frac{\beta}{4\tau}\left(T_{\rm M}^4 - T_0^4\right). \tag{6}$$

In view of the exponential-like decrease (respectively increase) of the temperature towards its saturation value in the S-zone (resp. N-zone), *generalized healing lengths* $z_{\rm S}$ and $z_{\rm N}$ can be defined in consistency with the former $\eta_{\rm S}$ and $\eta_{\rm N}$ of the STD model.

B. Thermal and Electrical Parameters for a Nb Strip

We will choose the case of Nb sample FK-91 ($b = 80$ nm; $w = 10$ μm; $T_{\rm c} = 8.6$ K) studied in [5]. From its resistivity $\rho(10$ K$) = 2.68$ $\mu\Omega$.cm, the electron diffusivity $D_e = 30$ cm^2.s^{-1} follows. The phonon thermal conduction can be omitted in the heat transport along the filament.

Little is known about the heat capacities in thin films. So it is convenient to rely on data gathered on the bulk material. In the superconducting and the normal states, one can introduce the three components $C_{\rm eS}$, $C_{\rm eN}$, and C_ϕ according to:

$$C_{\rm S}(T) = \mu T^3(\text{electrons}) + \beta T^3(\text{phonons}) \tag{7a}$$

$$C_{\rm N}(T) = \gamma T(\text{electrons}) + \beta T^3(\text{phonons}). \tag{7b}$$

In the useful temperature range, the choice $\gamma = 705$ J.m^{-3}.K^{-2}; $\beta = 12.45$ J.m^{-3}.K^{-4}; $\mu = 26.5$ J.m^{-3}.K^{-4}, provides a satisfactory representation with accuracy better than 2%, apart for $C_{\rm eS}$ in the range 0 to 3 K, of minor importance [5].

C. Phonon Escape Time

Our choice $(\beta/4\tau)[T^4 - T_0^4]$ to express the power, per unit volume of the filament, transferred to the substrate, seems reasonable, insofar as the characteristic time τ or phonon escape time can be reached. In fact, it has been discovered by Pals and Wolter [6], and later developed by Tinkham [7], that the nucleation time of phase-slip centers, the precursors of the current-induced HSs, follows a law derived from a time-dependent Ginzburg-Landau equation, with a relaxation time $\tau_{\rm d}$ (d for its relationship with delay time) as a scaling parameter.

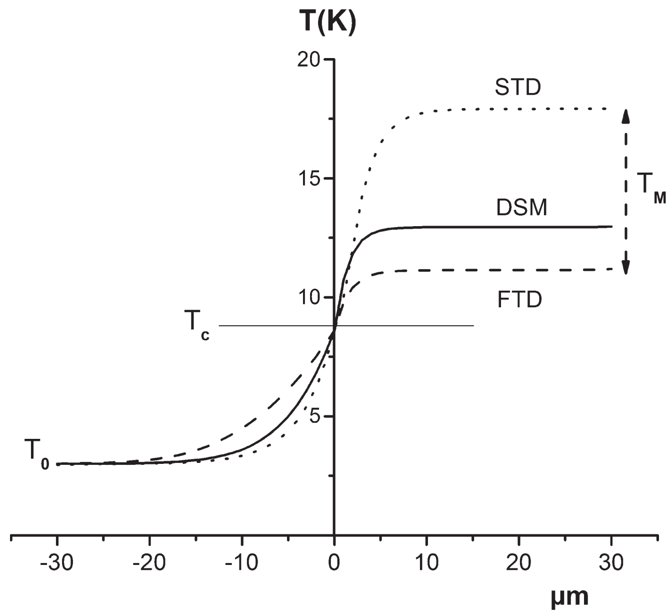

Fig. 2. Predictions of the three models STD, DSM, and the present one FTD using the same mode of computation and the same set of parameters. $T_0 = 3$ K. T_{M} are 17.90, 12.95, and 11.15 K, respectively. On the S side, the three traces stand in the reverse order, compared to the N side.

At least in two cases, that of Nb strips (cf. Appendix in [5]) and of YBCO strips [8], this τ_{d} could be identified with the film cooling time. Knowing the total and the phononic specific heats, C(T) and $C_{\mathrm{ph}}(T)$, it is straightforward to deduce the *experimental* value of the phonon escape time $\tau = (C_{\mathrm{ph}}/C)\,\tau_{\mathrm{d}}$. Over a large span of thicknesses and temperatures, the results could be expressed as a time per unit thickness: $\tau/b = 25$ ps/nm for Nb on Al_2O_3 [5], and $\tau/b = 75$ ps/nm for $YBa_2Cu_3O_7$ on MgO [8].

IV. Computational Methods and Departures From Previous Treatments

We look for the T-profile of a permanent hot spot of length $L_{\mathrm{n}} \gg (\eta_{\mathrm{S}}, \eta_{\mathrm{N}})$, standing far from the extremities of a strip of length $L \gg L_{\mathrm{N}}$, in thermal contact with a substrate cooled at T_0. The differential system (5a), (5b) was solved numerically (Equation Solver, Mathematica). In practice, for a given T_0, a trial value is given to the derivative $(dT_{\mathrm{S}}/dx)_{x=0}$, and a temperature function T(x) develops in the S zone ($x < 0$). The requirement of monotonicity is sufficient to define very accurately a unique $(dT_{\mathrm{S}}/dx)_{x=0}$, and eventually the full function $T_{\mathrm{S}}(x)$.

From that point and on, the N-zone function $T_{\mathrm{N}}(x > 0)$ is computed according to (5b) with the boundary condition $dT/dx = 0$ at infinity on the N side. Such a solution is obtained after giving several trial values to T_{M}, again guided by the monotonicity of $T_{\mathrm{N}}(x)$, wherefrom a well-defined value of the parameter T_{M} emerges.

In order to enlighten the consequences of the present FTD model, we plot in Fig. 2 the results corresponding to STD, DSM, and FTD, using the same thermal parameters. One notes (a) an obvious kink in the T-profile at the S/N junction; (b) the deep penetration of the temperature wave into the S-region, compared to the "linear" healing length $\eta_{\mathrm{S}} = 3.5$ μm; and (c) a shorter normal state healing length. The contrast between DSM and FTD results mainly from the term in $(dT/dx)^2$ in the heat balance equations being of the same sign as d^2T/dx^2 (upward curvature) in the S-region, but of the opposite sign in the N region (downward curvature).

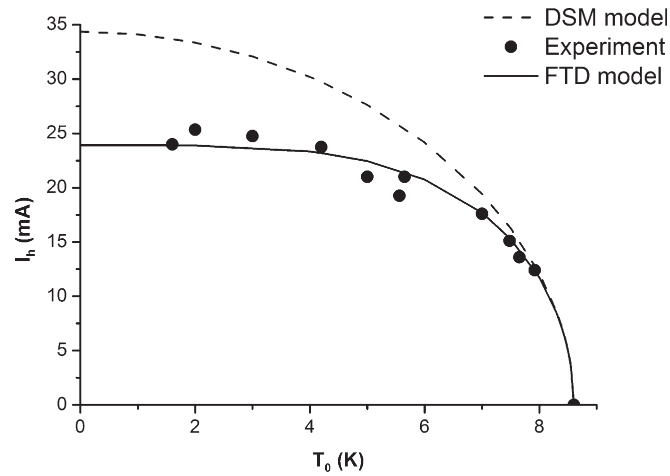

Fig. 3. HS minimum current in niobium FK-91 versus bath temperature T_0, according to the DSM model (upper trace) and to the present FTD model. Full circles are data deduced from pulse experiments [5].

V. Comparison With Experimental HS Currents $I_{\mathrm{h}}(T_0)$

In most investigations about HS in thin strips, I_{h} is defined as the so-called retrapping current measured in dc conditions. In the case of Sample FK-91, it was obtained [5] as the current that maintains a constant value of the voltage as the driving current is reduced from an exciting pulse of large amplitude. These data were taken in pulse conditions to avoid substrate heating. Thus experimental determinations of $I_{\mathrm{h}}(T_0)$, down to $T_0 \sim 0.2T_{\mathrm{c}}$ are available for comparison with theory.

In Fig. 3, theoretical traces, DSM and FTD, computed with the *same set of parameters*, are plotted together with the experimental $I_{\mathrm{h}}(T_{\mathrm{c}})$. (Let us note that the latter are affected by an uncertainty typical of pulse determinations). Obviously, the FTD model fits the experimental I_{h}, while the DSM model leads to too large HS currents. That disagreement is aggravated in the STD model, due to the absence of the blackbody coupling term.

VI. Application to a Nanometer-Thin NbN Filament

Strips of nanometric thickness have become widespread in the recently developed [1] Superconducting Single Photon Detectors (SSPDs). Let us take the NbN filament described in [9], and adapt the parameter values to the present terminology. Those are: $b = 6$ nm; $\rho = 268$ $\mu\Omega$.cm; $D_{\mathrm{e}} = 0.45$ cm^2.s^{-1}; $T_{\mathrm{c}} = 10$ K; $\beta = 9.8$ J.m^{-3}.K^{-4}; $\gamma = 240$ J.m^{-3}.K^{-2}; $\tau/b = 13$ ps/nm. The electronic specific heat C_{eS} not being specified in [9], we manage to choose it in the same ratio with γT_{c}

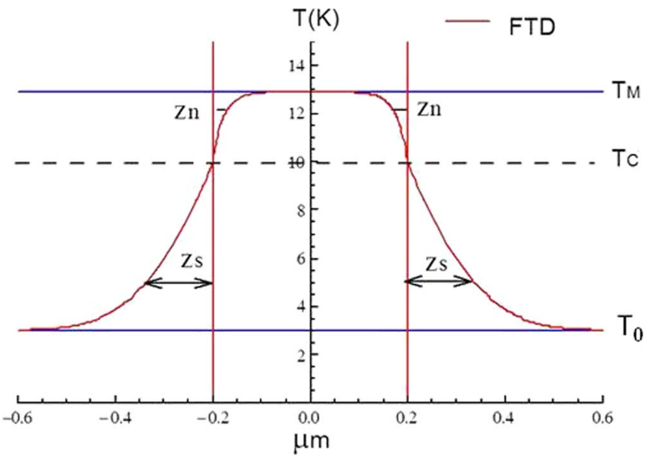

Fig. 4. Calculated temperature profile of a steady HS in a NbN strip, 6 nm thick. Parameters are specified in [9]. Bath temperature $T_0 = 3$ K. Top temperature $T_{\mathrm{M}} = 12.9$ K. The healing lengths $\mathrm{Z_S}$ and $\mathrm{Z_N}$ appear much shorter than in the Nb case (cf Fig. 2).

as for Nb, which leads to $\mu = 6.25$ J.m^{-3}.K^{-4}. The resulting temperature profile is shown in Fig. 4, where the main features are the much shorter healing lengths compared to Nb strips, due to the poor electron diffusivity of ultrathin NbN strips, and the top temperature $T_{\mathrm{M}} = 12.9$ K for $T_0 = 3$ K.

The HS current density derived from this T_{M} is 1.95 MA.cm^{-2}. Unfortunately, that quantity does not appear in [9]. Work in progress in our laboratory tends to yield longer values of τ/b than 13 ps/nm. A direct measurement of I_{h} would discriminate between these different estimates.

Finally, as it has been pointed out by Marsali *et al.* [10], the one temperature approximation is questionable in ultrathin strips, as the escape time τ may become shorter than $\tau_{\mathrm{p-e}}$, the equilibration time of the phonons with the electron gas. That is unlikely to occur in NbN strips, due to the short value of $\tau_{\mathrm{p-e}}$. For the Nb films considered in the present work, the confinement of the phonons, or phonon bottleneck ($\tau > \tau_{\mathrm{p-e}}$), results from a larger thickness (80 nm) of our samples.

VII. Conclusion

By taking full account of the non-linear heat flux equations through the interface, and of the blackbody phonon radiation, we have computed the T-profile of a self-heating hotspot, and deduced the corresponding stabilizing current. In a niobium strip, the latter is in close agreement with the measurements even far from the critical temperature. The temperature elevation appears significantly lower than predicted by previous models.

The method was applied to a fictitious steady hotspot in a NbN filament a few nanometer thick.

References

[1] G. N. Gol'tsman, O. Okunev, G. Chulkova, A. Lipatov, A. Semenov, K. Smirnov, B. Voronov, A. Dzardanov, C. Williams, and R. Sobolewski, "Picosecond superconducting single-photon optical detector," *Appl. Phys. Lett.*, vol. 79, p. 705, 2001.

[2] W. J. Skocpol, M. R. Beasley, and M. Tinkham, "Self-heating hotspots in superconducting thin-film microbridges," *J. Appl. Phys.*, vol. 45, p. 4054, 1974.

[3] S. Yamasaki and T. Aomine, "Self-heating effects in long superconducting thin films over a wide temperature range," *Jpn. J. Appl. Phys.*, vol. 18, p. 667, 1979.

[4] G. Dharmadurai and N. S. Satya Murthy, "A simplified expression for the minimum hotspot current in long, thin-film superconductors," *J. Low Temp. Phys.*, vol. 37, p. 269, 1979.

[5] F.-R. Ladan, K. Harrabi, M. Rosticher, C. Villard, P. Mathieu, and J.-P. Maneval, "Current-temperature diagram of resistive states in long superconducting niobium filaments," *J. Low Temp. Phys.*, vol. 153, p. 103, 2008.

[6] J. A. Pals and J. Wolter, "Measurement of the order-parameter relaxation in superconducting Al-strips," *Phys. Lett. A*, vol. 70, p. 150, 1979.

[7] M. Tinkham, "Heating and dynamic enhancement in metallic weak links," in *Non-Equilibrium Superconductivity, Phonons and Kapitza Boundaries*, K. E. Gray, Ed. New York: Plenum, 1981, pp. 231–262.

[8] K. Harrabi, N. Cheenne, F. Boyer, F. Chibane, P. Delord, F.-R. Ladan, and J.-P. Maneval, "Thermal boundary resistance of $YBa_2Cu_3O_7$ on MgO deduced from the transient V(I) response," *Supercond. Sci. Technol.*, vol. 13, p. 1222, 2000.

[9] A. D. Semenov, G. N. Gol'tsman, and A. Korneev, "Superconducting nanowire single-photon detector," *Phys. C*, vol. 351, p. 349, 2001.

[10] F. Marsili, F. Najafi, C. Herder, and K. Berggren, "Electrothermal simulation of superconducting nanowire avalanche photodetectors," *Appl. Phys. Lett.*, vol. 98, p. 093507, 2011.